ICARUS 75, 171–184 (1988)

# Sources and Distribution of Odd Nitrogen in the Venus Daytime Thermosphere

J.-CL. GÉRARD, E. J. DENEYE, AND M. LERHO

*Institut d'Astrophysique, Université de Liège, B-4200 Ougrée-Liège, Belgium*

Received May 11, 1987; revised October 28, 1987

**A photochemical-diffusive model of the Venusian dayside ionosphere is developed to study the distribution of atomic nitrogen and nitric oxide above 100 km and the supply of N atoms to the nightside. The model is validated by comparing the calculated ion and electron density with the measurements of the ion mass spectrometer on board the Pioneer-Venus Orbiter. The model shows little sensitivity to the value of the efficiency of the $N(^2D)$ production by $N_2$ dissociation and $N(^2D)$ quenching coefficient by atomic oxygen. The calculated $N(^4S)$ is in good agreement with the vertical distribution and local time dependence observed with the Pioneer-Venus neutral mass spectrometer above 150 km. A maximum concentration of about $8 \times 10^7$ cm$^{-3}$ is predicted at 124 km near 1700 local time. The average amount of nitrogen atoms globally produced on the dayside is estimated to $1.3 \times 10^{10}$ cm$^{-2} \cdot$ sec$^{-1}$. Comparison of this source with the emission rate of the nitric oxide recombination nightglow measured with the Pioneer-Venus Orbiting Ultraviolet Spectrometer indicates that about 50% of the nitrogen atoms are transported to the nightside by the thermospheric general circulation.** 

## INTRODUCTION

The discovery with the Pioneer-Venus Orbiting Ultraviolet Spectrometer (PV-OUVS) of the nitric oxide chemiluminescent emission on the nightside of Venus (Stewart and Barth 1979, Stewart *et al.* 1980, Gérard *et al.* 1981) substantiated the concept of a thermospheric day-to-night circulation previously introduced in hydrodynamical models (Dickinson and Ridley 1977). According to this view, the initial source of nightside oxygen and nitrogen atoms is on the dayside where they are directly or indirectly produced by dissociation of $CO_2$ and $N_2$. However, no detailed model of dayside odd nitrogen sources and sinks and their solar zenith angle dependence has been developed so far. A preliminary study of the neutral and ion odd nitrogen chemistry was made by Rusch and Cravens (1979), soon after the first Pioneer Venus results were available. Reasonably good agreement with observations was obtained for ionic species with the exception of $N^+$ ions. Their model predicted that ground state $N(^4S)$ atoms were the major neutral odd nitrogen species, with a peak concentration of about $2 \times 10^7$ cm$^{-3}$ near 130 km. However, no atomic nitrogen measurements were available for comparison with the model predictions.

Based on preliminary estimates of the dayside atomic nitrogen production rate and of the nitric oxide nightglow intensity, Rusch and Cravens concluded that the sunlit thermospheric source is adequate to provide the necessary flux of nitrogen atoms to the nightside. This conclusion was challenged by Krasnopolsky (1983), who, on the basis of a simplified model, concluded that virtually the total dayside production of N atoms would be required on the nightside to account for the NO recombination airglow.

Reexamination of this problem is clearly needed, taking into account the abundant data base on neutral and ionic densities col-



0019-1035/88 $3.00

lected during the first 3 years of the PV Orbiter mission. For this purpose, we developed a photochemical-diffusive model of the Venusian daytime ionosphere and odd nitrogen. Crucial tests of the validity of this model are obtained by comparing the calculated atomic nitrogen vertical profile and local time distribution with the $N(^4S)$ measurements obtained with the PV neutral mass spectrometer (PV-ONMS) (Kasprzak *et al.* 1980, Niemann *et al.* 1980). Such a comparison is useful, not only as a model validation, but also to evaluate the validity of current odd nitrogen photochemistry in a $CO_2$-dominated atmosphere. Finally, the results of these detailed photochemical calculations could be used in future three-dimensional hydrodynamical models to parameterize the sources and sinks of atomic nitrogen in the Venus sunlit thermosphere.

## THE MODEL

### *1. Description*

The temperature and number density distribution of the major constituants ($CO_2$, CO, O, and $N_2$) are taken from the empirical thermospheric model by Hedin (1983), based on the Neutral Mass Spectrometer on board the PV Orbiter (Niemann *et al.* 1980). This model includes a correction by a factor 1.63 to the ONMS absolute densities introduced to reconcile the total density with that derived from drag measurements (Hedin *et al.* 1983). However, it is not clear whether a common correcting factor should be applied to all individual densities measured by the ONMS (Keating *et al.* 1985). The input parameters for this model are the $F10.7$-cm solar flux, the Ap magnetic index, latitude, and local solar time. Below 120 km, the density profiles are extrapolated downward assuming hydrostatic equilibrium and using the temperature profile from Keating *et al.* (1985).

The coupled continuity and diffusion equations are solved for $N(^4S)$, $N(^2D)$, and NO. Photochemical equilibrium equations are solved for $CO_2^+$, $CO^+$, $O_2^+$, $O^+(^4S)$, $O^+(^2D)$, $O^+(^2P)$, $N_2^+$, $N^+$, $NO^+$, and electrons. Neglect of vertical transport for the ions restricts the validity of the computed ionosphere to altitudes up to about 200 km, where diffusive and chemical lifetimes become approximately equal for $O^+$ and $N^+$ ions. Molecular and turbulent vertical diffusion is included for odd nitrogen species using the expressions given by Banks and Kockarts (1973) and von Zahn *et al.* (1980), respectively. A zero flux condition is used for all three species at the upper (200 km) and lower (80 km) boundaries of the model.

The electron temperature profiles are obtained from the Theis *et al.* (1980) empirical model down to 130 km. Below this altitude, the electron temperature is smoothly connected to the neutral temperature and both values are equal below 120 km. The time-dependent second-order system of partial differential equations for odd nitrogen is solved using the numerical method described by Hastings and Roble (1977). The total integration time is chosen so that a steady-state solution is obtained.

The unattenuated ionization frequencies of $CO_2$, CO, $N_2$, and O and their dependence on the $F10.7$-cm solar flux are taken from the calculations by Torr and Torr (1985), using a linear interpolation between the solar maximum and minimum sets of values. The effective absorption and ionization cross sections by Torr *et al.* (1979) are adopted to calculate the vertical distribution of the ion production rates. The calculation of the photoelectron flux and $N_2$ dissociation will be discussed below.

Most rate coefficients adopted in this study are identical to those used by Fox (1982) in her model of the Venusian ionosphere. However, some of them have been updated, based on recent determinations. Others, not experimentally determined, have been modified to improve the agreement between measured and calculated concentrations. For example, the rate of the charge-exchange reaction between metastable $O^+(^2D)$ and $N(^4S)$ ($R_7$; see Table I) has been doubled with respect to the

TABLE I

| Reaction number | | Rate ($cm^3$ $sec^{-1}$) |
|---|---|---|
| | Photochemical processes | |
| $P_1$ | $N_2 + h\nu(e) \rightarrow N_2^+ + e(+e)$ | $I_1$ |
| $P_2$ | $\rightarrow N^+ + N + e(+e)$ | $I_2$ |
| $P_3$ | $N + h\nu \rightarrow N^+ + e$ | $I_3$ |
| $P_4$ | $NO + h\nu \rightarrow NO^+ + e$ | $I_4$ |
| $P_5$ | $N_2 + h\nu \rightarrow N + N$ | $J_1$ |
| $P_6$ | $N_2 + e \rightarrow N + N + e$ | $J_2$ |
| $P_7$ | $\rightarrow N^+ + N + 2e$ | $J_3$ |
| $P_8$ | $NO + h\nu \rightarrow N(^4S) + O$ | $J_4$ |
| | Chemical reactions | |
| $R_1$ | $N_2^+ + e \rightarrow N(^2D) + N(^4S)$ | $1.8 \times 10^{-7} \left(\frac{T_e}{300}\right)^{-0.4}$ |
| $R_2$ | $NO^+ + e \rightarrow N(^2D,^4S) + O$ | $4.2 \times 10^{-7} \left(\frac{T_e}{300}\right)^{-0.85}$ |
| $R_3$ | $N_2^+ + O \rightarrow NO^+ + N(^2D)$ | $1.4 \times 10^{-10} \left(\frac{T}{300}\right)^{-0.44}$ |
| $R_4$ | $O^+ + N_2 \rightarrow NO^+ + N(^4S)$ | $1.5 \times 10^{-12}$–$5.9 \times 10^{-13} \left(\frac{T}{300}\right)$ |
| $R_5$ | $O^+(^2P) + N_2 \rightarrow N^+ + NO$ | $1.3 \times 10^{-10}$ |
| $R_6$ | $\rightarrow N_2^+ + O$ | $1.4 \times 10^{-10}$ |
| $R_7$ | $O^+(^2D) + N(^4S) \rightarrow N^+ + O$ | $3 \times 10^{-10}$ |
| $R_8$ | $N^+ + CO_2 \rightarrow CO^+ + NO$ | $2.5 \times 10^{-10}$ |
| $R_9$ | $N^+ + CO \rightarrow CO^+ + N$ | $4 \times 10^{-10}$ |
| $R_{10}$ | $\rightarrow NO^+ + C$ | $5.4 \times 10^{-11}$ |
| $R_{11}$ | $N^+ + O \rightarrow O^+ + N(^4S)$ | $2.2 \times 10^{-12}$ |
| $R_{12}$ | $N^+ + NO \rightarrow NO^+ + N(^4S)$ | $8 \times 10^{-10}$ |
| $R_{13}$ | $N(^2D) + CO_2 \rightarrow NO + CO$ | $6.8 \times 10^{-13}$ |
| $R_{14}$ | $N(^2D) + O^+ \rightarrow N^+ + O$ | $1.3 \times 10^{-10}$ |
| $R_{15}$ | $N(^2D) + O_2^+ \rightarrow N^+ + O_2$ | $4 \times 10^{-10}$ |
| $R_{16}$ | $N(^2D) + NO \rightarrow N_2 + O$ | $6.3 \times 10^{-11}$ |
| $R_{17}$ | $N(^2D) + O \rightarrow N(^4S) + O$ | $5 \times 10^{-13}$ |
| $R_{18}$ | $N(^2D) + CO \rightarrow N(^4S) + O$ | $2.5 \times 10^{-12}$ |
| $R_{19}$ | $N(^2D) + e \rightarrow N(^4S) + e$ | $2.7 \times 10^{-13} T_e$ |
| $R_{20}$ | $N(^2D) + CO_2^+ \rightarrow N^+ + CO_2$ | $2 \times 10^{-10}$ |
| $R_{21}$ | $N(^2D) \rightarrow N(^4S) + h\nu$ | $1.07 \times 10^{-5}$ $sec^{-1}$ |
| $R_{22}$ | $N(^4S) + NO \rightarrow N_2 + O$ | $3.4 \times 10^{-11}$ |
| $R_{23}$ | $N(^4S) + CO_2^+ \rightarrow NO^+ + CO$ | $1 \times 10^{-11}$ |
| $R_{24}$ | $N(^4S) + CO^+ \rightarrow NO^+ + C$ | $2 \times 10^{-11}$ |
| $R_{25}$ | $N(^4S) + O_2^+ \rightarrow NO^+ + O$ | $1.8 \times 10^{-10}$ |
| $R_{26}$ | $NO + O_2^+ \rightarrow NO^+ + O_2$ | $4.4 \times 10^{-10}$ |
| $R_{27}$ | $NO + N^+ \rightarrow NO^+ + N(^4S)$ | $3.3 \times 10^{-10}$ |
| $R_{28}$ | $NO + CO_2^+ \rightarrow NO^+ + CO_2$ | $1.2 \times 10^{-10}$ |
| $R_{29}$ | $NO + CO^+ \rightarrow NO^+ + CO$ | $3.3 \times 10^{-10}$ |

value used by Fox (1982), in order to improve the agreement with the measured $N^+$ profile. The charge transfer process

$$O^+ + H \rightarrow O + H^+$$

has a rate coefficient of $2.2 \times 10^{-11}$ $T_i^{0.5}$ (Nagy *et al.* 1980) and the similar reaction with $O^+(^2D)$,

$$O^+(^2D) + H \rightarrow O + H^+,$$

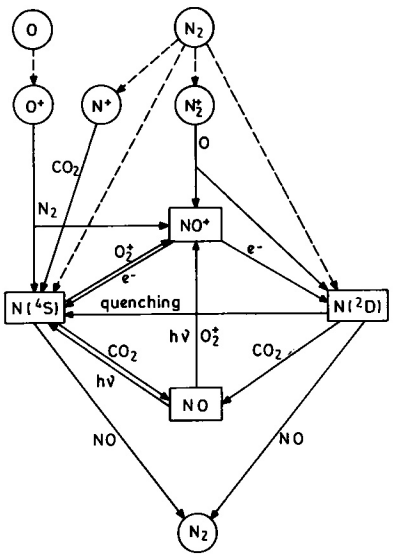


FIG. 1. Block diagram of odd nitrogen sources and sinks in the Venusian thermosphere. The dotted lines indicate nonthermal ionization and dissociation processes.

was assumed to be three times as fast, although the reaction with ground-state $O^+$ is resonant and thus not likely to be faster with metastable atoms. Inclusion of these sinks of $O^+$ ions is important for large solar zenith angles, when atomic hydrogen is large and prevents the calculated density from exceeding the experimental values. The profile of atomic hydrogen and its dependence on solar zenith angle is adopted from Keating *et al.* (1985).

Of particular importance in the context of this study is the modeling of processes controlling the odd nitrogen chemistry. Figure 1 shows a simplified reaction scheme describing the dominant processes effecting odd nitrogen. For the sake of understandability, the reactions involving metastable $O^+$ and the detailed processes controlling the $N^+$ ions are not indicated in the figure. Defining the odd nitrogen family as the sum of the N($^4$S), N($^2$D), NO, $NO^+$, and $N^+$ densities, the sources of odd nitrogen in the Venus thermosphere are processes $P_1$, $P_2$, $P_5$, $P_6$, $P_7$, $R_1$, $R_3$, $R_4$, and $R_5$. Its destruction is due solely to reactions $R_{16}$ and $R_{22}$.

When this scheme is compared to that controlling thermospheric odd nitrogen on Earth (Gérard and Taieb, 1986), the major processes are seen to be very similar. The main difference is that, in the near absence of oxygen on Venus, the role of $O_2$ on Earth is played by $CO_2$ on Venus. This difference affects mostly the internal partitioning between odd nitrogen species, but the initial steps in the production of odd nitrogen (breaking of an $N_2$ bond) are accomplished through the same processes on both planets.

Three long-lived levels of atomic nitrogen (N($^4$S), N($^2$D), N($^2$P)) are produced by dissociation of $N_2$. However, the main N($^2$P) loss process is radiative deexcitation which populates the N($^2$D) and, to a minor extent, the N($^4$S) states through emission in the 1046- and 520-nm doublets (Fox 1982). Consequently, we prefer to use an effective branching ratio for the combined net production of N($^2$D) and N($^2$P) atoms rather than introduce a third species whose production is largely unknown and which only acts as a transit energy reservoir.

The dissociation of $N_2$ by electron impact ($P_6$),

$$N_2 + e \rightarrow N + N + 2e,$$

and the dissociative ionization of $N_2$ ($P_7$),

$$N_2 + e \rightarrow N^+ + N + 2e,$$

may produce nitrogen atoms in the three low-energy states of N. Predissociation of $N_2$ by ultraviolet photons ($P_5$),

$$N_2 + h\nu \rightarrow N + N,$$

may also be a significant source of nitrogen atoms (Hudson and Carter 1969, Zipf and McLaughlin 1978). In this study, following the suggestion by Richards *et al.* (1981), we assume that all solar photons absorbed by $N_2$ in the 80- to 100-nm range lead to a predissociation of the molecule. Based on measurements of the excitation cross section of $N_2$ into singlet valence and Rydberg states, Zipf and McLaughlin (1978) argued that about 50% of the atoms are created by

$P_6$ in the $^4S$ state; the remaining 50% are shared between the $^2D$, $^2P$, and higher lying states. However, studies of the Earth's atomic nitrogen emissions (Rusch *et al.* 1975, Frederick and Rusch 1977) and nitric oxide distribution (Gérard *et al.* 1986, Ogawa *et al.* 1984) require a $N(^2D)$ branching ratio of at least 60% for processes $P_5$ and $P_6$. We use this efficiency as a standard value in this model. However, in a subsequent section, this assumption is shown to be of minor consequence for the Venus odd nitrogen modeling.

Laboratory measurements of the quenching of $N(^2D)$ atoms by atomic oxygen ($R_{17}$) have yielded coefficients of about $2 \times 10^{-12}$ $cm^3 \cdot sec^{-1}$ at room temperature. These values are substantially larger than those derived by Frederick and Rusch (1977) from the analysis of the 520-nm $N(^2D)$ terrestrial airglow. The importance of the choice between these two values is evaluated below.

*2. Photoelectron Flux*

The calculation of the photoelectron flux is based on the method described by Richards and Torr (1983). The photoelectron fluxes deduced from this method for the Earth's atmosphere were compared by Richards and Torr to more detailed calculations and Atmosphere Explorer-E measured spectra. They were found to be in satisfactory agreement, considering the uncertainties in both measurements and energy loss cross sections.

In this method, local energy deposition is assumed and use is made of the concept of average energy loss per collision. In this approximation, the flux at energy $E$ is given by

$$\Phi(E) = \frac{P(E) + Q(E)}{\sigma_{N_2}(E) + \sigma_O(E) + \sigma_{CO_2}(E) + \sigma_{CO}(E) + L_e(E)}$$

where $P(E)$ and $Q(E)$ denote the primary and cascading secondary productions at energy $E$, $\sigma_{N_2}$, $\sigma_O$, $\sigma_{CO_2}$, and $\sigma_{CO}$, the total inelastic cross sections for electron impact on $N_2$, O, $CO_2$, and CO, and $L_e(E)$ the loss function to thermal electrons.

TABLE II

| Photoelectron energy (eV) | Average energy loss (eV) | |
|---|---|---|
| | $CO_2$ | CO |
| 0–8 | 1 | |
| 8–15 | 8, 10, 12 | 6, 8, 10 |
| 15–100 | 11, 13, 15 | 10, 12, 14 |

The value of $Q(E)$ is obtained by associating an average energy loss with each energy bin of the primary electron spectrum $P(E)$ for each major constituent. The choice of the average energy loss per collision is based on the energy of the excited states of each neutral species but is somewhat arbitrary. In the case of $N_2$ and O, the values determined by Richards and Torr were adopted. For $CO_2$ and CO, the energy losses are listed in Table II. They are based on the excitation and ionization cross sections given by Jackman *et al.* (1977). The branching ratios for the production of the various levels of $CO_2^+$ given by Mantas and Hanson (1979) were adopted. For sake of simplicity, all $CO^+$ ions are assumed to be created in the $X^2\Sigma^+$ ground state. As in the case of the Earth's thermosphere, we verified that the final energy spectra remained relatively insensitive to the choice of these values.

Since no detailed experimental photoelectron spectra are available for Venus, we compared our calculated spectra to theoretical and observed fluxes for Mars, whose thermosphere is similar in atmospheric composition. Figure 2 shows a comparison of the fluxes calculated for Mars at 130 km for a solar zenith angle of 45° by Fox and Dalgarno (1979) and by the method described before, using the same model atmosphere. Both the absolute fluxes and the shapes of the two curves are in good agreement. The minor slight differences observed in the amplitude of the

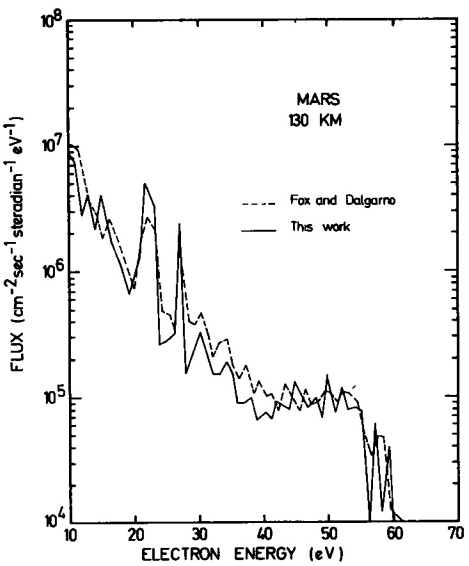


FIG. 2. Photoelectron energy spectrum calculated for Mars at 130 km using the average energy loss concept. The flux calculated by Fox and Dalgarno (1979) for the same neutral atmosphere is plotted in dashed line for comparison.

peaks at 22, 30, and 34 eV is due mostly to the use of somewhat different solar ultraviolet irradiances and cross sections. Consequently, we feel that this simplified method also provides reliable evaluations of the photoelectron energy spectrum in the Venus thermosphere.

The ionization rates of the ambient atoms and molecules and the dissociation rate of $N_2$ by electron impact are obtained by integrating the photoelectron flux over the relevant cross section. In the case of the $N_2$ dissociation, the total cross section measured by Zipf *et al.* (1980), which is in good agreement with Winters' (1966) and Niehaus' (1967) values, is used. We use an efficiency of 0.6 for the $N(^2D)$ effective production by electron impact dissociation of $N_2$ for our standard model. This value is somewhat larger than 0.5 derived by Zipf *et al.* (1980) by combining theoretical considerations with airglow measurements. The branching ratio adopted for the production of electronically excited N atoms by processes $P_1$ and $R_1$ is 50% in both cases.

### *3. Model Validation*

Since the model described before will be used to infer the vertical distribution, the diurnal variation, and the total production rate of odd nitrogen species, it is important to first validate it. This may be done by comparing the ionospheric and $N(^4S)$ concentrations yielded by the calculations to a sample of measurements made with the Pioneer Venus instrumentation.

*a. Ionosphere.* First, we consider the electron density and ion composition. Figures 3a and 3b show the comparison between the calculated profile of ions and the measurements made during the ascent of orbit 185 for $O^+$, $CO_2^+$, the sum $CO^+ + N_2^+$, $NO^+$, $N^+$, and the electron density $N_e$. The positive ion concentrations were measured with the Orbiter Ion Mass Spectrometer (OIMS) during the upleg for a solar zenith angle of 11° at a mean latitude of 5°N (Taylor *et al.* 1980). The various instruments measuring directly or indirectly (by summing the positive ions) the electron density are in fair agreement above 200 km. However, below this altitude, the OIMS total ion density trends to depart from the other measurements. Miller *et al.* (1984) showed that for solar zenith angles about 55°, the OIMS value exceeds the other measurements by a factor as large as 2.5, possibly as an effect of dynamical processes in this region. We have adopted the vertical $N_e$ profile from Miller *et al.* (1984), for comparison in Fig. 3. The average peak value measured from the radio occultation for this period of the mission (Kliore 1984, in Bauer *et al.* 1985) has also been plotted with its error bar. The profiles calculated from our standard model for SZA = 0° are in general good agreement with the measurements, considering the instrumental uncertainties and the intrinsic variability of the Venus ionosphere (Taylor *et al.* 1981). This electron density profile reproduces well the observations from the peak (140 km) to the top of the model. The total $O^+$ (sum of $O^+(^2P)$, $O^+(^2D)$, and $O^+(^4S)$) closely

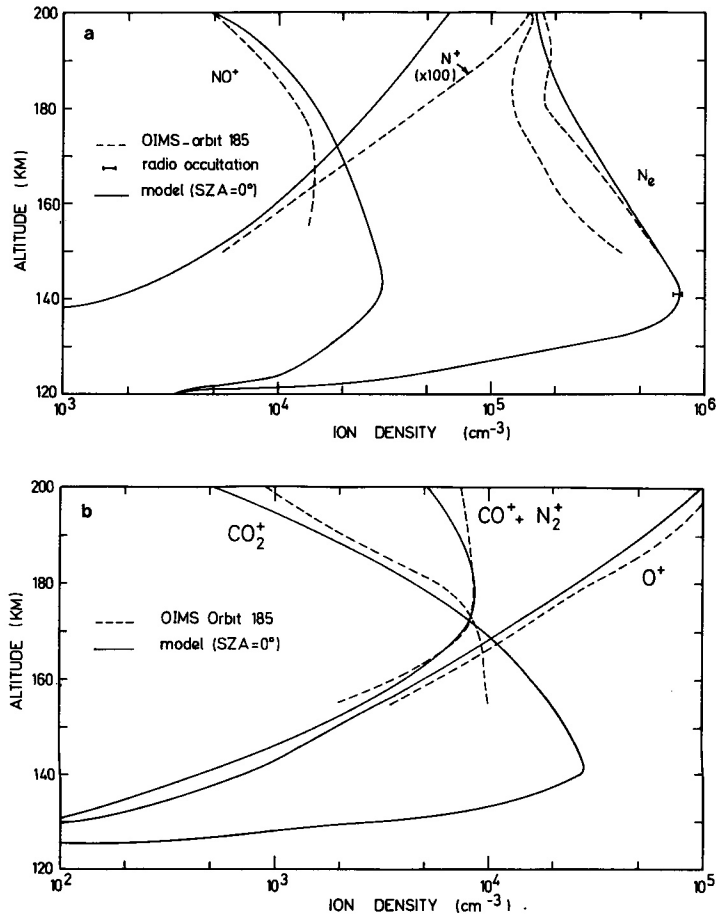


FIG. 3. Calculated ionic composition and comparison with the OIMS measurements on the upleg of Pioneer-Venus orbit 185. (a) $NO^+$, $N^+$, and $N_e$. (b) $O^+$, $CO_2^+$, $CO^+$, + $N_2^+$.

matches the measured concentration. Similarly, mass 28 ($CO^+$ + $N_2^+$) and $CO_2^+$ and $NO^+$ above 170 km are in excellent agreement with the OIMS values. Below this altitude, the measured [$CO_2^+$] and [$NO^+$] abruptly change slope, a feature not predicted by our model nor observed with the RPA (Miller *et al.* 1984). The $N^+$ is in good agreement with measurements at low altitude but is underestimated by a factor of 3 near 200 km.

The overall agreement is satisfactory and has been verified with measurements made at other solar zenith angles and latitudes. In particular, the calculated magnitude and height of the electron density peak follows very closely the dependence deduced by Kliore from the radio occultation measurements (Bauer *et al.* 1985).

The calculated local time dependence for equatorial latitudes of the $O^+$, $O_2^+$, $NO^+$, and $N^+$ concentrations at 200 km is illustrated in Fig. 4. For comparison, the solar zenith angle dependence is measured with the OIMS (Taylor *et al.* 1981). Here again, the agreement may be considered as satisfactory, considering the variability of the individual ion concentrations. For example, the fairly flat response of the observed $N^+$ diurnal variation is in contrast with the decrease near the terminators observed in the other ion densities. The model correctly

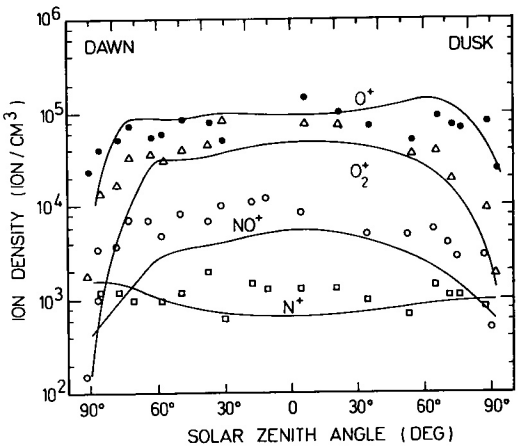


FIG. 4. Calculated and observed (Taylor *et al.* 1981) solar zenith angle dependence of $O^+$ (●), $O_2^+$ (△), $NO^+$ (○), and $N^+$(□).

predicts this difference in behavior. The absolute magnitudes of the ion concentrations also compare favorably with the modeled values with the exception of $NO^+$, which tends to be underestimated by the model.

*b. Atomic nitrogen.* The concentration of $N(^4S)$ atoms in the thermosphere has been determined with the ONMS instrument using the signal measured at mass 30. Kasprzak *et al.* (1980) described the measurements in some detail and showed the vertical distribution of atomic nitrogen measured on the downleg portion of PV orbit 205 above 160 km. These uncorrected measurements are displayed in Fig. 5, together with the vertical distribution calculated with our standard model. The measurements were made at 13.9 local time with a solar zenith angle of 32.5°. Also plotted are the vertical distributions of $N(^4S)$ calculated with our standard model for a solar zenith angle of 30° in the afternoon sector. The agreement with the measured density points is very good. The neutral atmospheric scale height associated with this curve is 21 km, corresponding to a local temperature of 305°K. This value should be compared with the 277°K derived by Kasprzak *et al.* (1980) from the scale height of the signal ascribed to atomic nitrogen.

Figure 6 illustrates the local time variation of the $N(^4S)$ density measured with ONMS in the altitude range 166–168 km during the first Venus year of the PV mission (Kasprzak *et al.* 1980, Niemann *et al.* 1980). The scatter observed in the data is a combination of the 2-km altitude range, differences in latitude of the measurements, and actual temporal variations. A plot at 157 km by Niemann *et al.* shows essentially the same characteristics.

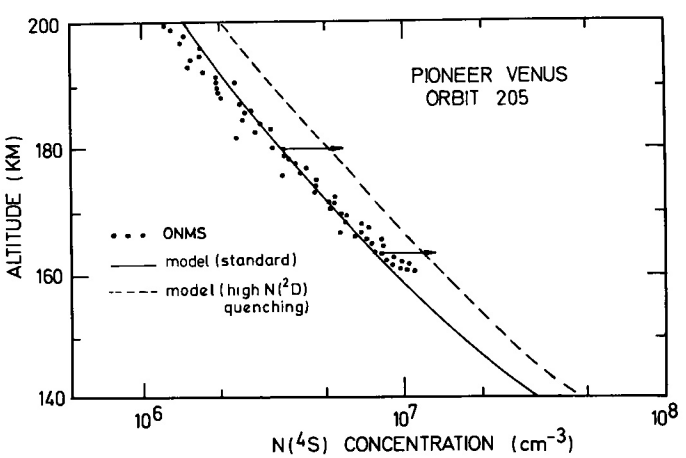


FIG. 5. Vertical distribution of $N(^4S)$ concentration calculated with the standard model (solid line) and with the alternative model (dotted line) for a solar activity index $F10.7$ cm = 200 and a solar zenith angle of 30°. The distribution measured by Kasprzak *et al.* (1980) is indicated by dots.

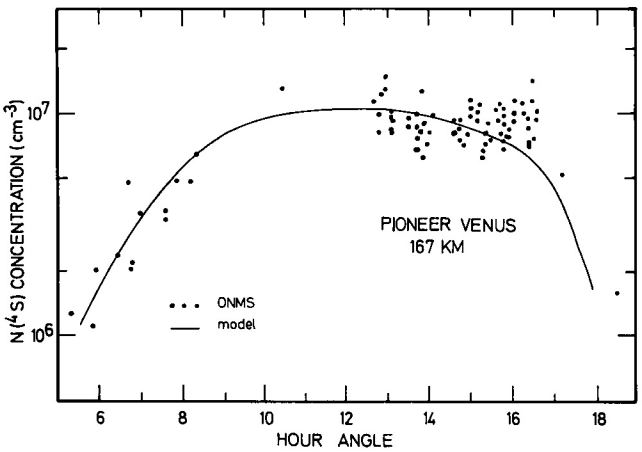


FIG. 6. Hour angle dependence of the N(⁴S) concentration calculated at 167 km with the standard model. The dependence measured by Niemann *et al.* (1980) with the ONMS is represented by dots.

The hour angle dependence predicted by this model at the same altitude for equatorial latitudes is shown as a solid line. Both the absolute value and the local time dependence are well predicted by the model calculations, although the small number of data points near the evening terminator makes quantitative comparisons in this sector speculative. The asymmetry observed in the morning and afternoon sectors is well reproduced by the model. However, the observed N(⁴S) distribution is rather flat between noon and 14.00 hr. This discrepancy may possibly be caused by dynamic effects of the interhemispheric thermospheric circulation.

## MODEL SENSITIVITY

The calculated vertical distribution of the three odd nitrogen species (N(⁴S), N(²D), NO) is represented for equatorial latitudes and 16.00 local time in Fig. 7. Ground-state atomic nitrogen is dominant in the range of altitude considered here. Its distribution reaches a peak of $6 \times 10^7$ cm$^{-3}$ at 126 km. Above 150 km, the density drops with a diffusive equilibrium scale height. Nitric oxide is the second most abundant species but remains over an order of magnitude below atomic nitrogen. A maximum of nearly $3 \times 10^6$ cm$^{-3}$ is obtained at 137 km. Finally, metastable N(²D) atoms exhibit a broad peak near 150 km and dominate over NO above 160 km. Above 180 km, the N(²D) distribution is in diffusive equilibrium with the same scale height as N(⁴S).

Most of the cross sections and rate coefficients used in this model were measured in

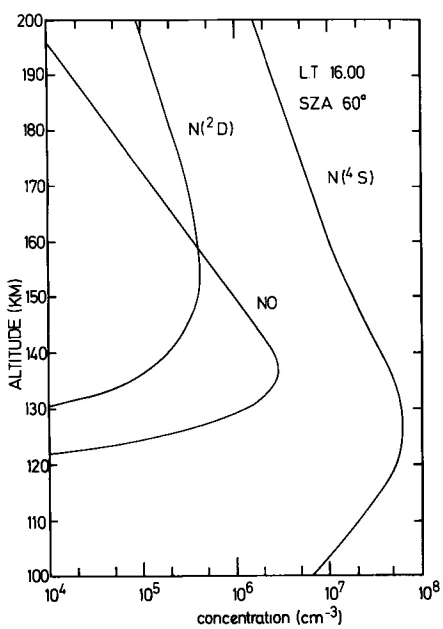


FIG. 7. Vertical distribution of N(⁴S), N(²D), and NO calculated at the equator for a local time of 16.00.

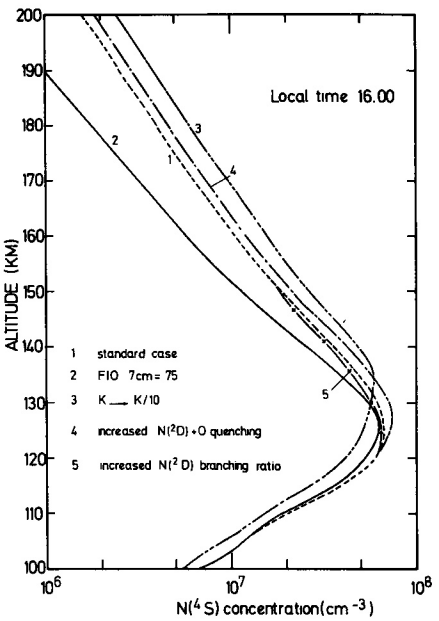


FIG. 8. Vertical distribution of N(⁴S) calculated under various assumptions at the equator for a local time of 16.00.

the laboratory or derived from satellite studies of the Earth's ionosphere and airglow. However, the value of some of them are still debated and it is important to test the sensitivity of the calculated distribution to the assumptions made concerning those values. Figure 8 illustrates the results of different parameter sensitivity studies.

Curve 1 is identical to the N(⁴S) curve in Fig. 6 and was obtained for a value of the $F10.7$ cm solar flux index of 150. Curve 2 is calculated with the same set of parameters but for a $F10.7$ cm index of 75, typical of solar minimum conditions. This lower solar activity affects both the temperature and vertical distribution of the major constituents and the solar ultraviolet irradiances. The high altitude distribution shows a smaller scale height than the standard model, corresponding to a drop in the exospheric temperature from 315 to 260°K. The peak value is only slightly affected as a result of the smaller absorption of solar EUV radiation by the overlying atmosphere at low solar activity. Curve 3 shows the sensitivity to the eddy diffusion coefficient. It is obtained by dividing the profile of $K$ values by a factor of 10 at all altitudes. As may be expected, this decrease in the strength of eddy mixing moves the altitude of the peak upward and decreases the atomic nitrogen density below the maximum. Consequently, the N(⁴S) density is larger by about 50% above 140 km.

The role of N(²D) deactivation by atomic oxygen (reaction $R_{17}$) is illustrated by curve 4. The quenching coefficient is set to $2 \times 10^{-12}$ cm$^3$ sec$^{-1}$, in agreement with laboratory determinations (Davenport *et al.* 1976, Iannuzzi and Kaufman 1980). The value of $4 \times 10^{-13}$ cm$^{-3}$ sec$^{-1}$ used in the standard model was derived from the analysis of the 520-nm airglow distribution measured with the AE-C satellite in the Earth's thermosphere (Frederick and Rusch 1977). It is seen that the choice of this coefficient, which is critical in the N–NO mutual equilibrium in the Earth's thermosphere, is of less consequence for N(⁴S) on Venus. This weaker sensitivity stems from the fact that reactions $R_{13}$ and $R_{18}$ dominate over $R_{17}$ at the peak of the N(⁴S) density.

Finally, the branching ratio of the production of N(²D) by $N_2$ dissociation ($P_5$, $P_6$) was increased from 0.6 to 0.7 (curve 5). This change has only minor effects on atomic nitrogen between 120 and 150 km. This result is again in contrast with the behavior of the thermospheric odd nitrogen system in the terrestrial atmosphere where this branching ratio critically controls the net production of nitric oxide and the [NO]/[N] ratio.

Consequently, the N(⁴S) photochemistry on Venus appears relatively well understood and suitable to model satisfactorily the observations. The calculated distribution is also much more independent of two parameters whose values play a critical role in the Earth's odd nitrogen modeling. For these two reasons, this model may be used confidently to predict the odd nitrogen distribution in regions or in conditions not yet accessed by *in situ* measurements.

The degree of agreement obtained with the dayside mass-spectrometer measurements is difficult to evaluate precisely since the correcting factor to apply to the $N(^4S)$ density is not unambiguously determined. The use of the high ($2 \times 10^{-12}$ cm$^3$ sec$^{-1}$) quenching coefficient of $N(^2D)$ by O, together with a 50% branching ratio for $P_5$ and $P_6$, increases the $N(^4S)$ profile above 140 km by 35% over the standard case (dotted line in Fig. 5). In this case, the atomic nitrogen peak remains nearly unchanged ($6.7 \times 10^7$ cm$^{-3}$ at 16.00 hr) but rises to $9.6 \times 10^6$ at 167 km.

## LOCAL TIME DEPENDENCE

The diurnal variation of atomic nitrogen was measured by the PV-ONMS instrument and studied at different altitudes above 160 km. However, the maximum of the atomic nitrogen production and the peak of $N(^4S)$ are located at altitudes below the PVO periapsis. Therefore, this model is used to predict the local time (or solar zenith angle) dependence of the nitrogen atom production and concentration.

Figure 9 shows the vertical profiles of $N(^4S)$ calculated with the standard model for various local times and 0° latitude. As time increases from early morning until noon, the $N(^4S)$ density increases steadily above 140 km. However, between 130 and 115 km, the sign of the variations reverses and the peak value at noon is about 30% less than at 17.00 local time (LT). During afternoon hours, the model predicts an increase of the peak density and a decrease of the atomic nitrogen concentration at high altitudes. The densities of atomic nitrogen are asymmetric; larger values are predicted in the afternoon than in the morning for a given solar zenith angle. This is a consequence of the local time asymmetry of the temperature and major neutral composition fields. The formulation adopted for the vertical dependence of the eddy diffusion coefficient ($K = An^{-1/2}$) is another source of coupling between the major neutral constituents and the $N(^4S)$ density.

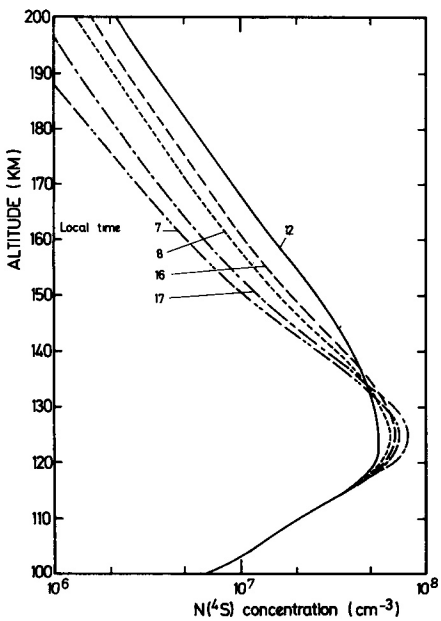


FIG. 9. Local time variation of the atomic nitrogen distribution calculated at the equator with the standard model.

The peak density of $N(^4S)$ is calculated for a solar zenith angle of 70° and reaches about $7.5 \times 10^7$ cm$^{-3}$. This value is substantially larger than the maximum of $1.8 \times 10^7$ cm$^{-3}$ obtained by Rusch and Cravens (1979). The discrepancy between the two models may be ascribed in part to the use of a somewhat different (more complete) photochemistry including metastable species in this study. The neutral atmospheric densities are also different, resulting in a different production rate of atomic nitrogen. The agreement is better with the curve calculated by Fox (1982), who obtained a peak of about $4 \times 10^7$ cm$^{-3}$ at 127 km for a solar zenith angle of 15°. At noon at the equator, our model gives a maximum of $5.4 \times 10^7$ cm$^{-3}$ at 124 km. This small difference is probably due in part to the NO profile obtained by Fox which, as a result of the location of the lower boundary, overestimates the nitric oxide concentration below 140 km.

Our (and consequently previous models') atomic nitrogen concentrations at 150 km

(Fig. 9) are substantially less than those given in VIRA by Keating *et al.* (1985) which range from $4.65 \times 10^7$ cm$^{-3}$ at 1200 to $3 \times 10^7$ cm$^{-3}$ at 8.00 and 16.00 LT. The N($^4$S) Venus International Reference Atmosphere (Keating *et al.* 1986) profile is very close to that given by the Hedin *et al.* (1983) empirical model.

## SUPPLY OF NITROGEN ATOMS TO THE NIGHTSIDE

As stated before, it is important to calculate the total production of nitrogen atoms on the dayside of the planet and compare it to the flux of atoms required to account for the nitric oxide night airglow observed with Pioneer Venus. The average downward flux of N atoms $\phi_N$ carried to the nightside is related to the emission rate of the NO-δ airglow by the relation

$$N = \frac{4\pi\bar{I} \times 10^9}{F\varepsilon},$$

where $4\pi\bar{I}$ is the measured average emission rate (in kR) of the (0,1) NO δ-band on the nightside; $F$, the fraction of photons of the NO recombination airglow emitted in the (0,1) δ-band; and $\varepsilon$, the efficiency of the radiative N + O recombination as a loss of nitrogen atoms on the nightside.

We use $4\pi\bar{I} = 780$ R and $\varepsilon = 0.45$ (Stewart *et al.* 1980). The value of $F$ may be derived from the terrestrial NO airglow measurements by McCoy (1983), who obtained

$$\frac{I(\delta(0,1)}{I(\delta)} = 0.32$$

for the ratio of the 198-nm band to the total NO ($^2\Pi - X^2\Pi$) intensity. We combine this result with the fraction of photons radiated into the system

$$\frac{I(\delta)}{I(\mathrm{NO})} = 0.77$$

measured by McCoy (1983) and also consistent with the values derived by Sharp and Rusch (1981) (0.79) and by Groth *et al.* (1971) (0.77). These values lead to an estimate of $\phi_N = 7 \times 10^9$ cm$^{-2}$ sec$^{-1}$, somewhat less than the flux initially derived by Stewart *et al.* (1980), based on a lower value of $F$.

The total dayside production of atomic nitrogen is obtained by performing the hemispheric integral

$$P_N = \int P_N(r,\theta,\phi) r^2 d\theta d\phi dr,$$

where $P_N$ denotes the local production of N atoms at planetocentric altitude $r$, solar zenith angle $\theta$, and azimuth $\phi$. Using the values of $P_N$ provided by the standard model and denoting by $S$ the area of one Venus hemisphere ($2.4 \times 10^{18}$ cm$^2$), we obtain

$$P_N = 1.3 \times 10^{10} S = 3.1 \times 10^{28} \text{ atoms} \cdot \text{sec}^{-1}$$

with an uncertainty in the model calculation estimated to be about 25%. Comparing $P_N$ and $\phi_N$, the efficiency of the transfer to the nightside of nitrogen atoms created in the dayside thermosphere is estimated to be 50%. The remaining atoms are lost chemically, mostly through mutual destruction with NO. This loss may take place below the N($^4$S) peak in the dayside thermosphere where nitrogen atoms are carried by diffusive transport and destroyed in the N + NO reaction ($R_{22}$). Another (small) fraction of the atoms will suffer chemical reactions along their trajectories to the nightside (Massie *et al.* 1983).

The average column production rate calculated above is slightly larger than the previous estimates of $1.1 \times 10^{10}$ cm$^{-2}$ sec$^{-1}$ by Krasnopolsky (1983) and $4.5 \times 10^9$ cm$^{-2}$ sec$^{-1}$ by Rusch and Cravens (1979). The reasons for the larger value are tied to differences in the detailed treatment of the photochemistry. For example, other studies ignored the quenching of N($^2$D) by CO, a major source of N($^4$) atoms. Other differences such as a different background atmosphere and UV solar irradiances and our consideration of the metastable $O^+$ chemistry may also account for the higher N($^4$S) production rate obtained in this study.

## CONCLUSIONS

We have shown that current understanding of the odd nitrogen photochemistry in a $CO_2$-dominated atmosphere appears adequate to account for the measured distribution of atomic nitrogen in the dayside thermosphere of Venus. In particular, the agreement between the calculated hour angle dependence of $N(^4S)$ and the ONMS *in situ* measurements suggests that no major sources or sinks of atomic nitrogen are overlooked among the processes controlling the distribution of $N(^4S)$ and $N(^2D)$. The lack of *in situ* measurements of nitrogen below 150 km and of NO at any altitude restricts the comparison to one of the three odd nitrogen constituents.

The weak dependence of the results on the $N(^2D) + O$ quenching coefficient and effective branching ratio of the $N(^2D)$ production by $N_2$ dissociation does not allow us to solve the discrepancy between theoretical and laboratory data and the observations of NO in the Earth's thermosphere. A useful constraint on these values would be provided by future simultaneous measurements of $N(^2D)$, $N(^4S)$, and NO in the Venusian lower thermosphere.

The average production of nitrogen atoms on the dayside is estimated to about $1.3 \pm 0.3 \times 10^{10}$ atoms $\cdot$ cm$^{-2}$ $\cdot$ sec$^{-1}$. It is thus adequate to supply the nightside with the flux of N atoms required to account for the nitric oxide recombination airglow observed with the PV orbiter. A detailed treatment of this problem requires the use of a two- or three-dimensional model coupling the hydrodynamic day-to-night flow with photochemical production and loss of odd nitrogen. In this case, the N–NO mutual destruction, the dayside sink of atomic nitrogen will readjust to the new conditions and decrease so that the local loss of atoms will be partly replaced by the general circulation and nightside destruction. Due to the complexity of the atomic nitrogen chemistry, computer time limitations make it necessary to parameterize the sources and sinks, based on one-dimensional models such as this one.

## ACKNOWLEDGMENTS

One of us (JCG) is supported by the Belgian National Foundation for Scientific Research (FNRS). Financial support by FRFC Grant 2.4507-82 is also acknowledged.

## REFERENCES

BANKS, P. M., AND G. KOCKARTS 1973. *Aeronomy*. Academic Press, New York.

BAUER, S. J., *et al.* 1985. The Venus ionosphere. In *The Venus International Reference Atmosphere* (A. J. Kliore, V. I. Moroz, and G. M. Keating, Eds.). COSPAR–Pergamon, Elmsford, NY.

DAVENPORT, J. E., T. G. SLANGER, AND G. BLACK 1976. The quenching of $N(^2D)$ by $O(^3P)$. *J. Geophys. Res.* **81,** 12–16.

DICKINSON, R. A., AND S. W. BOUGHER 1986. Venus mesosphere and thermosphere. 1. Heat budget and thermal structure. *J. Geophys. Res.* **91,** 70–80.

DICKINSON, R. A., AND E. C. RIDLEY 1977. Venus mesosphere and mesosphere temperature structure. 2. Day–night variations. *Icarus* **30,** 163–178.

FOX, J. L. 1982. The chemistry of metastable species in the Venusian ionosphere. *Icarus* **51,** 248–260.

FOX, J. L., AND A. DALGARNO 1979. Ionization, luminosity, and heating of the upper atmosphere of Mars. *J. Geophys. Res.* **84,** 7315–7333.

FREDERICK, J. E., AND D. W. RUSCH 1977. On the chemistry of metastable atomic nitrogen in the F region deduced from simultaneous satellite measurements of the 5200A airglow and atmospheric composition. *J. Geophys. Res.* **82,** 3509–3517.

GÉRARD, J. C., A. I. F. STEWART, AND S. W. BOUGHER 1981. The altitude distribution of the Venus ultraviolet nightglow and implication on vertical transport. *Geophys. Res. Lett.* **8,** 633–636.

GÉRARD, J. C., AND C. TAIEB 1986. The E-region electron density diurnal asymmetry at Saint-Santin: Observations and role of nitric oxide. *J. Atmos. Terr. Phys.* **48,** 471–483.

GROTH, W., D. KLEY, AND V. SCHURATH 1971. Rate constants for the infrared emission of the NO ($C^2\Pi$-$A^2\Sigma^+$) transition. *J. Quant. Spectrosc. Rad. Transfer* **11,** 1475.

HASTINGS, J. T., AND R. G. ROBLE 1977. An automatic technique for solving coupled vector systems of non-linear parabolic partial differential equations in one space dimension. *Planet. Space Sci.* **25,** 209–215.

HEDIN, A. E., H. B. NIEMANN, W. T. KASPRZAK, AND A. SEIFF 1983. Global empirical model of the Venus thermosphere. *J. Geophys. Res.* **88,** 73–83.

HUDSON, R. D., AND V. L. CARTER 1969. Atmospheric implications of predissociation in $N_2$. *J. Geophys. Res.* **74,** 393–395.

IANNUZZI, M. P., AND F. KAUFMAN 1980. Rate of some reactions of N($^2$D and $^2$P) near 300 K $\phi$. *J. Chem. Phys.* **73,** 4701–4702.

JACKMAN, C. H., R. H. GARVEY, AND A. E. S. GREEN 1977. Electron impact on atmospheric gases. I. updated cross sections. *J. Geophys. Res.* **82,** 5081–5090.

KASPRZAK, W. T., A. E. HEDIN, H. B. NIEMANN, AND N. W. SPENCER 1980. Atomic nitrogen in the upper atmosphere of Venus. *Geophys. Res. Lett.* **7,** 106–109.

KEATING, G. M., *et al.* 1986. Models of Venus neutral upper atmosphere: Structure and composition. In *The Venus International Reference Atmosphere* (A. J. Kliore, V. I. Moroz, and G. M. Keating, Eds.). COSPAR–Pergamon, Elmsford, NY.

KRASNOPOLSKY, V. A. 1983. Lightning and nitric oxide on Venus. *Planet. Space Sci.* **31,** 1363–1370.

MANTAS, G. P., AND W. B. HANSON 1979. Photoelectron fluxes in the Martian ionosphere. *J. Geophys. Res.* **84,** 369–385.

MASSIE, S. T., D. M. HUNTEN, AND D. R. SOWELL 1983. Day and night models of the Venus thermosphere. *J. Geophys. Res.* **88,** 3955–3969.

MCCOY, R. P. 1983. Thermospheric odd nitrogen, 1, NO, N($^4$S) and O($^3$P) densities from rocket measurements of NO $\delta$ and $\gamma$ bands, the $O_2$ Herzberg I bands. *J. Geophys. Res.* **88,** 3197–3205.

MILLER, K. L., W. C. KNUDSEN, AND K. SPENNER 1984. The dayside Venus ionosphere. I. Pioneer Venus retarding potential analyzer experimental observations. *Icarus* **57,** 386–409.

NAGY, A. F., T. E. CRAVENS, S. G. SMITH, H. A. TAYLOR AND H. C. BRINTON 1980. Model calculations of the dayside ionosphere of Venus: Ionic composition. *J. Geophys. Res.* **85,** 7795–7801.

NIEHAUS, A. 1967. Anregung und dissoziation von molekülen beim elektrononbeschuss. *Z. Naturforsch.* **22**(a), 690.

NIEMANN, H. B., W. T. KASPRZAK, A. E. HEDIN, D. M. HUNTEN, AND N. W. SPENCER 1980. Mass spectrometric measurements of the neutral gas composition of the thermosphere and exosphere of Venus. *J. Geophys. Res.* **85,** 7817–7827.

OGAWA, T., N. IWAGANI, AND Y. KONDO 1984. Solar cycle variation of thermospheric nitric oxide. *J. Geomagn. Geoelectr.* **36,** 317–340.

RICHARDS, P. G., AND D. G. TORR 1983. A simple theoretical model for calculating and parameterizing the ionospheric photoelectron flux. *J. Geophys. Res.* **88,** 2155–2162.

RICHARDS, P. G., D. G. TORR, AND M. R. TORR 1981. Photodissociation of $N_2$: A significant source of thermospheric atomic nitrogen. *J. Geophys. Res.* **86,** 1495–1498.

RUSCH, D. W., AND T. E. CRAVENS 1979. A model of the neutral and ion nitrogen chemistry in the daytime thermosphere of Venus. *Geophys. Res. Lett.* **6,** 791–794.

RUSCH, D. W., A. I. STEWART, P. B. HAYS, AND J. H. HOFFMAN 1975. The NI (5200 Å) dayglow. *J. Geophys. Res.* **80,** 2300–2304.

SHARP, W. E., AND D. W. RUSCH 1981. Chemiluminescence of nitric oxide ($C^2\Pi$-$A^2\ \Sigma^+$) rate constant. *J. Geophys. Res.* **25,** 413–417.

STEWART, A. I. F. 1980. Design and operation of the Pioneer Venus Orbiter Ultraviolet Spectrometer. *IEEE Trans. Geosci. Remote Sensing* **GE-18,** 65.

STEWART, A. I., AND C. A. BARTH 1979. Ultraviolet night airglow of Venus. *Science* **205,** 59–62.

STEWART, A. I. F., J. C. GÉRARD, D. W. RUSCH, AND S. W. BOUGHER 1980. Morphology of the Venus ultraviolet night airglow. *J. Geophys. Res.* **85,** 7861–7870.

TAYLOR, H. A., S. J. BAUER, R. E. DANIELL, H. C. BRINTON, H. G. MAYR, AND R. E. HARTLE 1981. Temporal and spatial variations observed in the ionospheric composition of Venus: Implications for empirical modelling. *Adv. Space Res.* **1,** 37–51.

TAYLOR, H. A., H. C. BRINTON, S. J. BAUER, R. E. HARTLE, P. A. CLOUTIER, AND R. E. DANIELL 1980. Global observations of the composition and dynamics of the ionosphere of Venus: Implications for the solar wind interaction. *J. Geophys. Res.* **85,** 7765–7777.

THEIS, R. F., L. H. BRACE, AND M. G. MAYR 1980. Empirical models of the electron temperature and density in the Venus ionosphere. *J. Geophys. Res.* **85,** 7787–7794.

TORR, M. R., AND D. G. TORR 1985. Ionization frequencies for solar cycle 21: Revised. *J. Geophys. Res.* **90,** 6675–6678.

TORR, M. R., D. G. TORR, R. A. ONG, AND H. E. HINTEREGGER 1979. Ionization frequencies for major constituents as a function of solar cycle 21. *Geophys. Res. Lett.* **6,** 771–774.

VON ZAHN, U., K. H. FRICKE, D. M. HUNTEN, D. KRANKOWSKY, K. MAUERSBERGER, AND A. O. NIER 1980. *J. Geophys. Res.* **85,** 7829–7840.

WINTERS, H. F. 1966. Ionic absorption and dissociation cross section for nitrogen. *J. Chem. Phys.* **44,** 1472.

ZIPF, E. C., P. S. ESPY, AND C. F. BOYLE 1980. The excitation and collisional deactivation of metastable N($^2$P) atoms in auroras. *J. Geophys. Res.* **85,** 687–694.

ZIPF, E. C., AND R. W. MCLAUGHLIN (1978). On the dissociation of nitrogen by electron impact and by EUV photoabsorption. *Planet. Space Sci.* **26,** 449–462.